Progress In Electromagnetics Research C, Vol. 113, 83–96, 2021

A Dual Bandpass Filter Design Using Strong Coupling, Evanescent Mode and Modular Concept

Sek-Meng Sow*, Peng-Khiang Tan, and Jian Lu

Abstract—This paper presents a new design concept of a dual bandpass filter. Based on the strong coupling between two resonators, a dual 1-pole band-pass filter is designed and is used as the basic building block. By providing appropriate weak coupling between these building blocks, a higher-order dual bandpass filter can be realized. In addition, these building blocks can be stacked vertically and/or horizontally to construct a compact filter. In this way, by using 3D full wave EM and circuit co-simulation, the simulation time required in the design stage can be reduced. In addition, it also provides a way to post-tune each building block individually and further reduces the time required in prototype post tuning process. However, using this design approach, the band separation ratio is limited by the physically achievable coupling. For demonstration, an L-band dual 4-pole bandpass filter is designed with passband frequencies of 1.2 GHz $\sim$ 1.255 GHz and 1.55 GHz $\sim$ 1.6 GHz. To reduce the size of the filter and obtain a wide stopband bandwidth, a suitable evanescent mode cavity is used to realize the resonant structure. The measurement result shows that the insertion losses of the low passband and high passband are 1.03 dB $\sim$ 2.00 dB and 1.02 dB $\sim$ 1.75 dB, respectively; the return loss of both passbands is better than 15 dB. Furthermore, up to 5 GHz, the stopband rejection level is better than 80 dB.

1. INTRODUCTION

Microwave filters are an important component of modern wireless communication systems. Products with integrated multiple communication systems operating in different frequency bands are usually available in the market. Thus, filters with dual or multiple passbands are usually required to reduce the physical size and weight of a multi-system product. In addition, for high power applications, cavity filters are often used.

Generally, there are several methods that can be used to synthesize a single band filter (such as low pass, high pass, band-pass, or band-stop filters). They are image parameter method, insertion loss method [1], and coupling matrix method [2]. In addition, coupling matrix method is also used to synthesize filters with cross coupling between non-adjacent resonators to achieve transmission zero at the desired frequency.

For dual bandpass filter (DBPF) design, a simple method is to cascade the wide bandpass filter (BPF) with the stopband filter [3, 4]. However, the overall size of this DBPF is considered to be large. In order to achieve size reduction, several DBPF design techniques are suggested in [5–15]. [6] suggests to obtain a dual passband response by two BPFs coexisting in a single cavity, which is known as dual-path method. Since two sets of resonators are placed in a single cavity, in order to achieve good isolation between the paths, the cross-section of cavity is required to be larger, which may lead to spurious resonances in stopband. If a large stopband bandwidth is not required, this technique is suitable for tuneable DBPF design. In addition to the dual-path method, it is recommended to use

Received 25 March 2021, Accepted 4 June 2021, Scheduled 10 June 2021
* Corresponding author: Sek-Meng Sow (tslsowsm@nus.edu.sg).
The authors are with the Temasek Laboratories, National University of Singapore, Singapore.

dual resonance structures in DBPF design [10, 11] to excite two orthogonal resonance modes in the cavity, which is known as dual-mode method. By introducing multiple tuning screws into the dual-band dual-mode cylindrical cavity, a high-order DBPF can be constructed. The two disadvantages of this method are: 1) the size of the DBPF is inevitably large, and 2) the structure is complex. In addition to the dual-mode approach, coaxial Stepped-Impedance Resonators (SIRs) [5, 9], helical resonators [5], and iris windows [8, 12, 13, 15] are also recommended as dual resonances structures. The resonances of these structures are strategically designed to be located at the centre frequencies of the low passband and high passband of the DBPF. However, if the Band Separation Ratio (BSR, which is defined as ratio of the centre frequency of the upper passband, f_{c_HB}, to the centre frequency of the lower passband, f_{c_LB}) is low, the performance of the DBPF is very sensitive to the dimensional tolerance of the structure. Therefore, this type of DBPF is more suitable for applications that require a high BSR, such as a GSM/DCS cellular system with a BSR of 2. Other than structural methods, [7, 14] propose to obtain DBPF response based on the frequency transformation method [1]. In [7], the authors introduce a new frequency scaling factor (Eq. (1) of [7]) that can transform the Low Pass Filter (LPF) prototype into a DBPF prototype. For example, a simple 1-pole LPF consisting of a shunt capacitor is transformed into a DBPF, which consists of two LC parallel resonators and an admittance inverter between them. Generally, any of the above mentioned techniques can be selected to design DBPF according to the operating requirements of the application (such as size, power handling, and BSR).

Here, a novel technique for designing high-order DBPF is proposed. The high-order DBPF response is obtained by cascading multiple 1-pole DBPFs with appropriate weak couplings. These 1-pole DBPFs are regarded as basic building blocks and are designed based on the introduction of strong coupling between two resonators. For better power handling, it is recommended to build a 1-pole DBPF in an evanescent mode cavity with capacitive structures. The proposed design technique can be considered as a modular approach. In this way, using 3D full-wave EM/circuit co-simulation helps to shorten the design cycle. In addition, the 1-pole DBPF prototype can be examined individually, so the post tuning and troubleshooting time of the prototype can be further reduced. This type of DBPF is suitable for applications that need to operate under high power, low BSR, wide upper stopband bandwidth, and limited installation volume. In Section 2, the proposed modular design technique is introduced. A 4-pole DBPF is designed to demonstrate the proposed design technique, and the design process of the DBPF is also presented in Section 2. A prototype of the 4-pole DBPF is fabricated to verify the simulation results through experiments. Section 3 documents the measurement results of the prototype. Last but not least, Section 4 draws the conclusions of this paper.

In this work, all simulation results are obtained using CST Microwave Studio [16].

2. PROPOSED DESIGN TECHNIQUE

Generally, a single-band 2-pole BPF can be realized by two coupled resonators. The BPF can be represented by an admittance inverter ladders circuit, as shown in Figure 1(a). In addition, as shown in Figure 1(b), the admittance inverter can also be expressed as an inductive π-network [17]. The typical response of S_{11} and S_{21} of this filter is shown in Figure 2. Here, the interval between two resonances depends on the strength of the coupling or admittance inverter coefficient, $J_{1,2}$. If the coupling is weak, the two resonances are close to each other and form a 2-pole single-band BPF, as shown in Figure 2(a).

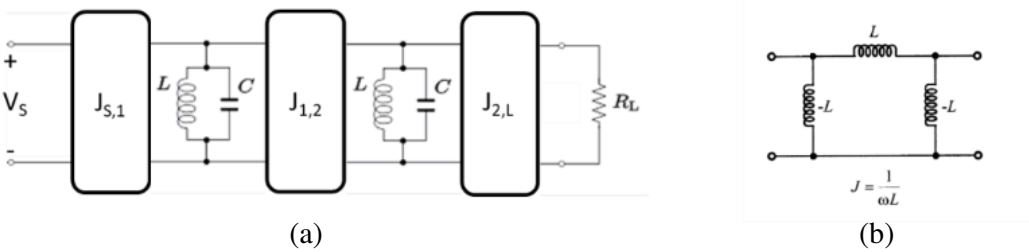

Figure 1. (a) An admittance inverter coupled 2-pole BPF circuit and (b) the equivalent lumped component circuit of an admittance inverter.

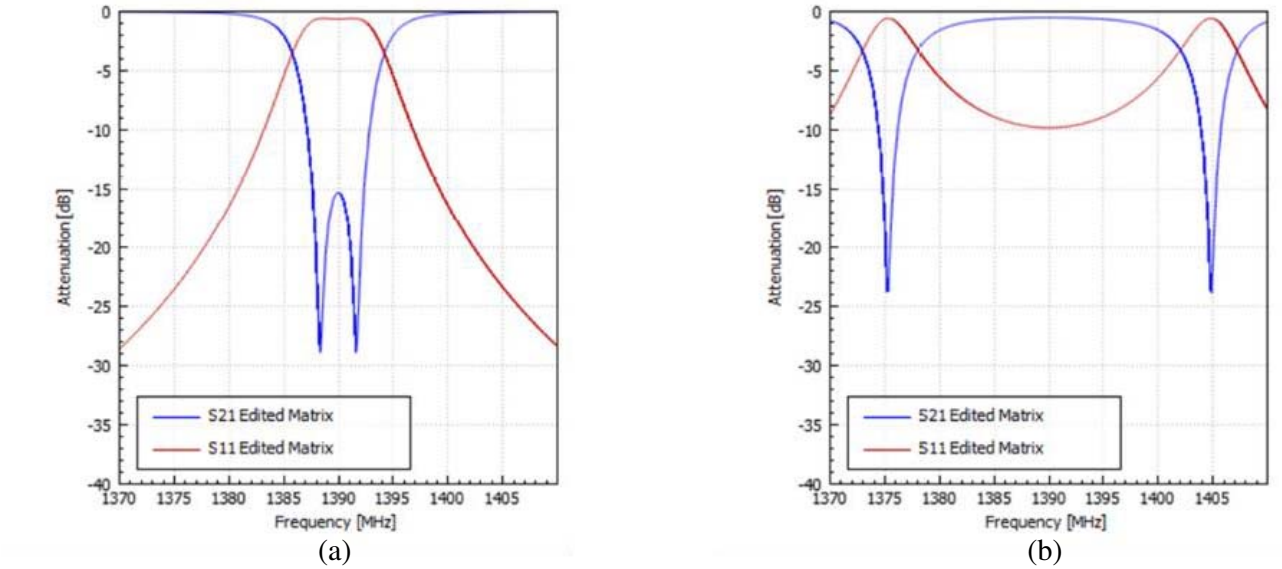

Figure 2. The S_{11} and S_{21} response of a 2-pole BPF with the (a) weak coupling and (b) strong coupling between two resonators.

On the other hand, as shown in Figure 2(b), a dual 1-pole BPF is realized by strong coupling between two LC resonators.

This dual 1-pole BPF is considered a dual-resonance structure and can be used as a basic building block for high-order DBPF. Using the same coupling concept explained in the previous paragraph, an N-order DBPF can be constructed by cascading N building blocks with weak coupling. For example, by using weak coupling, $J_{n-1,n}$, to connect two building blocks, a dual 2-pole BPF can be realized, as shown in Figure 3.

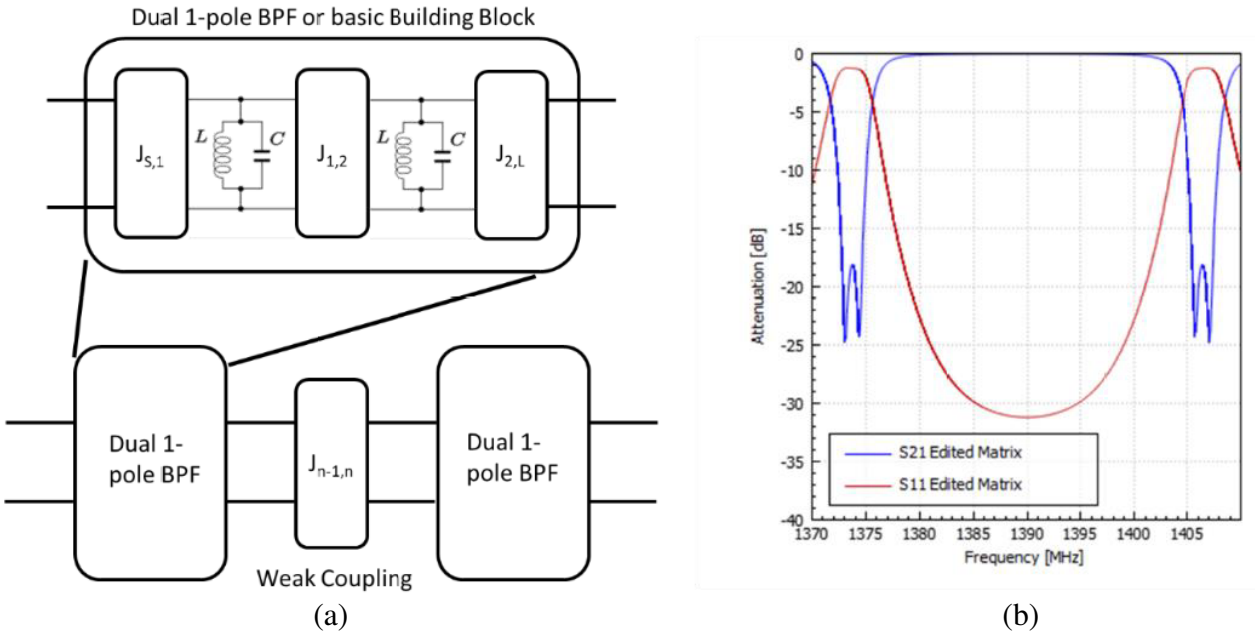

Figure 3. (a) A schematic diagram of a dual 2-pole BPF consists of 2 dual 1-pole BPFs with weak coupling between them. (b) The S_{11} and S_{21} responses of the dual 2-pole BPF.

2.1. Resonance Structure

The conventional microwave waveguide BPF has the characteristics of high power handling and low insertion loss. However, it usually comes in the form of bulky waveguide components. To overcome this problem, [17] suggests using evanescent-mode waveguide (EMW) to design waveguide filters. An EMW is a waveguide whose fundamental mode cutoff frequency is higher than the operating frequency. In this way, the overall size and weight of the BPF are greatly reduced. In addition, by choosing a suitable waveguide, the upper stopband of the filter can be extended up to 3× the centre frequency of the BPF. Therefore, it is recommended that the proposed DBPF uses the EMW to construct the resonator.

For detailed information on designing an EMW filter, one should refer to [17]. For brevity, only a quick introduction of EMW filter is given here. As shown in Figure 4, a short section of an EMW can be viewed as a π-inductive network [18]. The equivalent circuit can be mainly characterized by the size of the waveguide, and it is assumed that the only mode existing in the waveguide is the evanescent TE10 mode. Under this assumption, the equivalent circuit is valid for a BPF with a design bandwidth less than 20%.

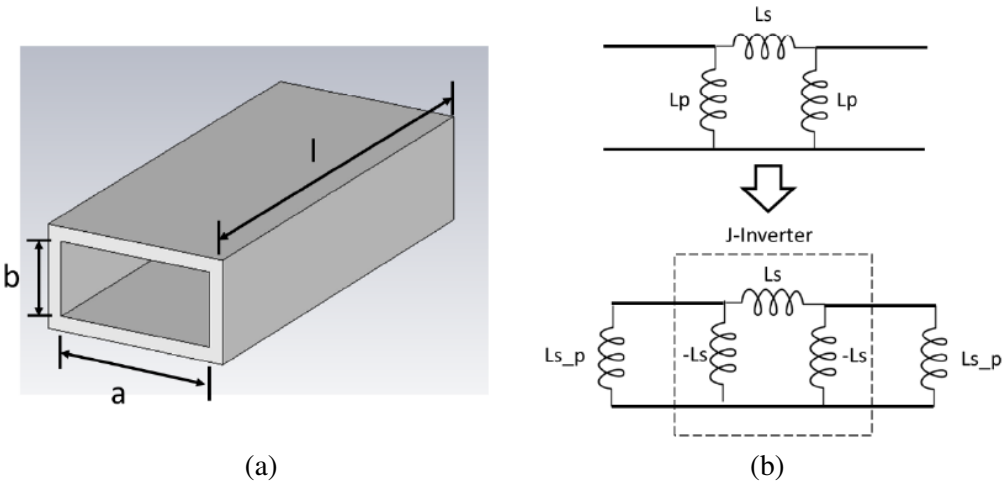

Figure 4. (a) An evanescent mode waveguide, where $2a <$ wavelength of the filter operating frequency and $a > b$, and (b) its equivalent π-inductive network.

As shown in Figure 4(b), the inductances, L_s and L_p, of the equivalent circuit are estimated based on the characteristic impedance, X_o, the propagation constant, γ, the lowest cutoff frequency of the EMW, f_c, the EMW size, a, b, l, and the operating frequency, f_o, using Eq. (1) and Eq. (2).

$$L_s = \frac{1}{\omega_o} X_o \sinh(\gamma l) \tag{1}$$

$$L_p = \frac{1}{\omega_o} X_o \coth\left(\frac{\gamma l}{2}\right) \tag{2}$$

where $X_o = \frac{120\pi b}{a\sqrt{\left(\frac{f_c}{f_o}\right)^2 - 1}}$, $\gamma = \frac{\omega_o}{c}\sqrt{\left(\frac{f_c}{f_o}\right)^2 - 1}$, $\omega_o = 2\pi f_o$.

In fact, as shown in Figure 4(b), the shunt inductor, L_p, of equivalent π-inductive network can be expressed by two shunt inductors, L_s and L_{s_p}, where $1/L_p = 1/L_{s\_p} - 1/L_s$. One should notice that the π-inductive network enclosed in the dotted box is actually equivalent to an admittance inverter with $J = 1/\omega L_s$. In this way, by using a short section of the EMW as a coupler between the resonators and treating the additional shunt inductance, L_{s_p}, as a part of the LC resonator, a BPF can be realized.

For example, by replacing the J inverter block with its equivalent π-inductive network, the lumped component equivalent circuit of a 2-pole BPF (as shown in Figure 1) can be drawn as Figure 5. This

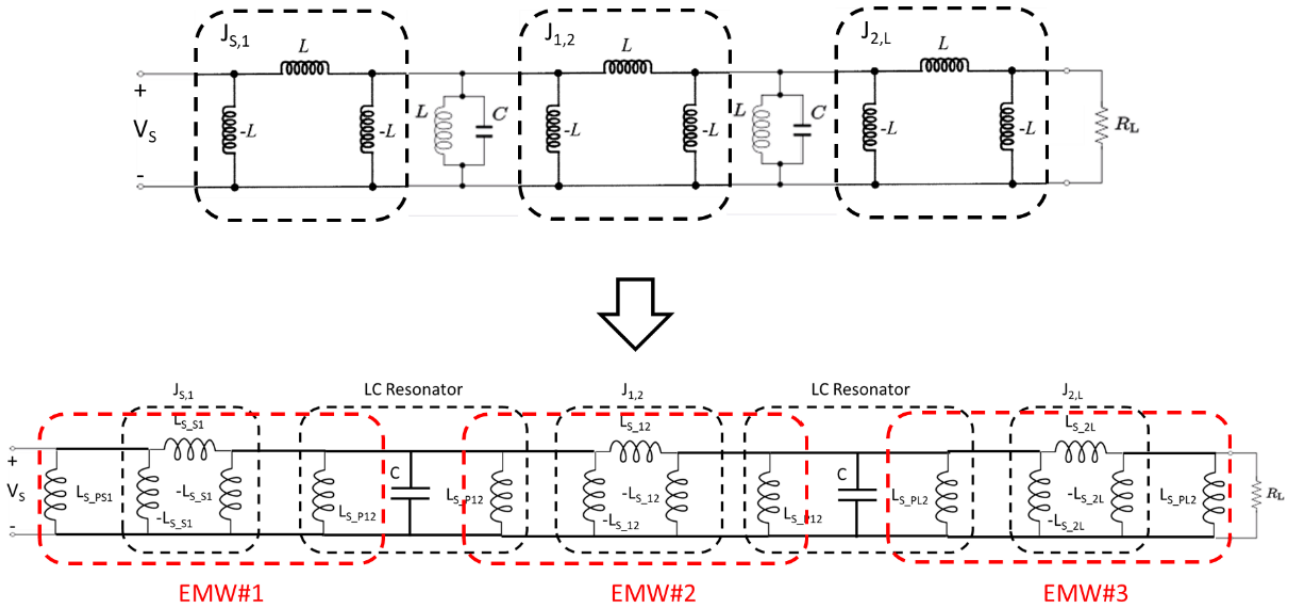

Figure 5. The schematic diagram of the 2-pole BPF with admittance inverters replaced by sections of EMW.

equivalent circuit can be implemented using three short sections of EMW and two capacitive structures. In general, a coaxial structure can be used as a capacitive structure. The detailed design of a rectangular capacitive structure is described in the design example section. As mentioned earlier, by increasing the coupling between the LC resonators, a 2-pole BPF becomes a dual 1-pole BPF. This dual 1-pole BPF is regarded as the basic building block of high-order DBPF.

2.2. Design Example: Dual 1-Pole BPF

To further illustrate the concept of using strong coupling for designing a Dual BPF, a simple dual 1-pole BPF is designed. The design requirement is as follows.

Parameter	Specification
Number of Poles for each passband	1
Low passband frequency	1227 MHz with BW of 0.5%
High passband frequency	1575 MHz with BW of 2%
Reflection Coefficient	< -15 dB

The coupling matrix of such a filter is obtained using the CST filter designer as follows, where "S" is referred as source, and "L" is load.

	S	1	2	L
S	0.000	0.354	0.000	0.000
1	0.354	0.000	1.007	0.000
2	0.000	1.007	0.000	0.354
L	0.000	0.000	0.354	0.000

The required resonance frequency of the resonator is the centre frequency between the two passbands, which is calculated as 1390 MHz. Here, the resonator is constructed using an EMW

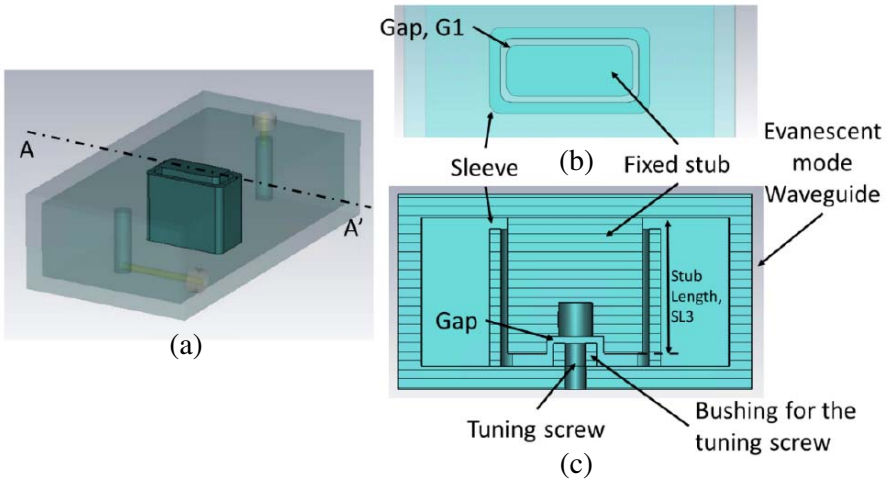

Figure 6. A rectangular coaxial structure. (a) 3D view, (b) top view and (c) AA' cross section view.

(27 mm × 13 mm) with a rectangular coaxial structure as the capacitive structure (as shown in Figure 6).

If the dimension of the sleeve and the EWM is 15 mm × 8 mm × 12 mm and 27 mm × 13 mm, respectively, the capacitance, C, of the rectangular coaxial structure can be estimated based on the gap, $G1$, and sleeve length, $SL1$ using an empirical formula stated in Eq. (3). A tuning screw is used to compensate any fabrication tolerance.

$$C = -8.3014 \times G1 + 0.5724 \times SL3 + 6.2446 \tag{3}$$

A complete design of the dual 1-pole BPF is shown in Figure 7. Using the coupling matrix and Eqs. (1) and (2), the initial length of the required EWG sections, $L1$, $L2$, and $L3$, are estimated as 5 mm, 8.1 mm, and 5 mm, respectively. Using these estimated lengths, the required inductance and capacitance of the parallel LC resonator are calculated as 1.61 nH and 8.16 pf, respectively. As such, using Eq. (3), the stub length, $SL3$, of the rectangular capacitive structure is estimated as 10.6 mm with

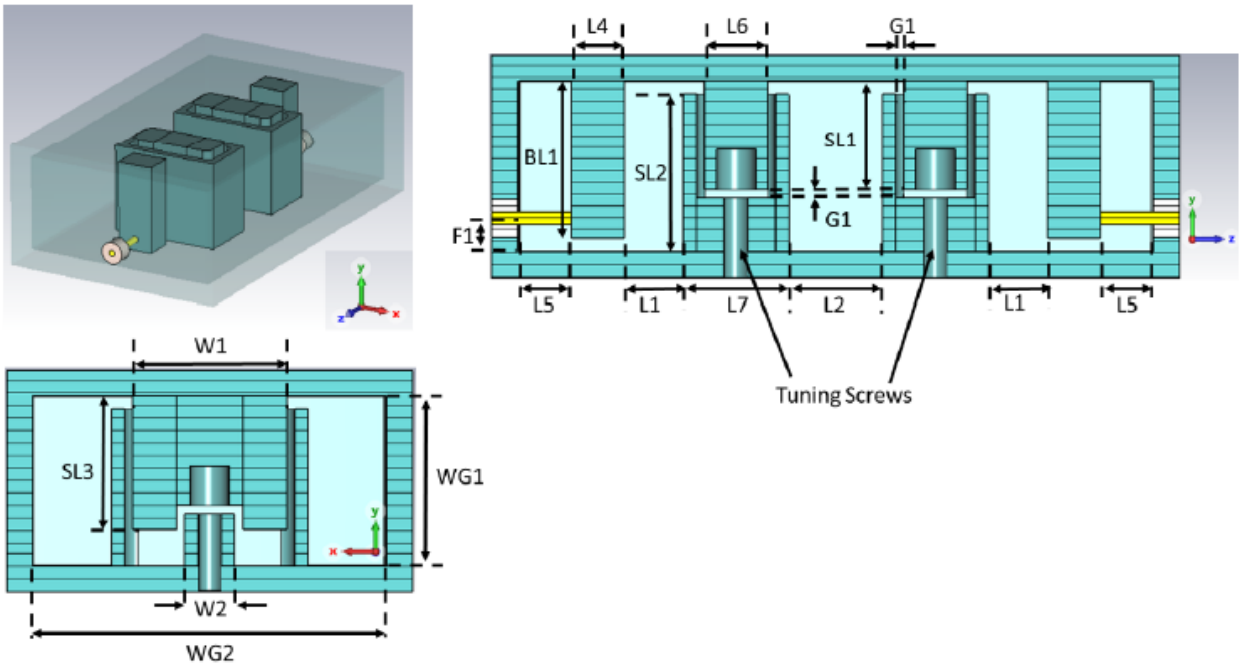

Figure 7. The structure of the dual 1-pole BPF.

a gap, $G1$, of 0.5 mm. However, these dimensions estimated based on the coupling matrix are only be used as initial values of the filter model. The optimized dimension of the dual 1-pole BPF is obtained as, $L1 = 4.5$ mm, $L2 = 7.1$ mm, $L4 = L5 = 4$ mm, $L6 = 4.8$ mm, $L7 = 8$ mm, $W1 = 15$ mm, $W2 = 5$ mm, $WG1 = 13$ mm, $WG2 = 27$ mm, $G1 = 0.6$ mm, $BL1 = 12.5$ mm, $SL1 = 8.3$ mm, $SL2 = 12$ mm and $SL3 = 11.1$ mm. The simulated S_{11} and S_{21} are shown in Figure 8.

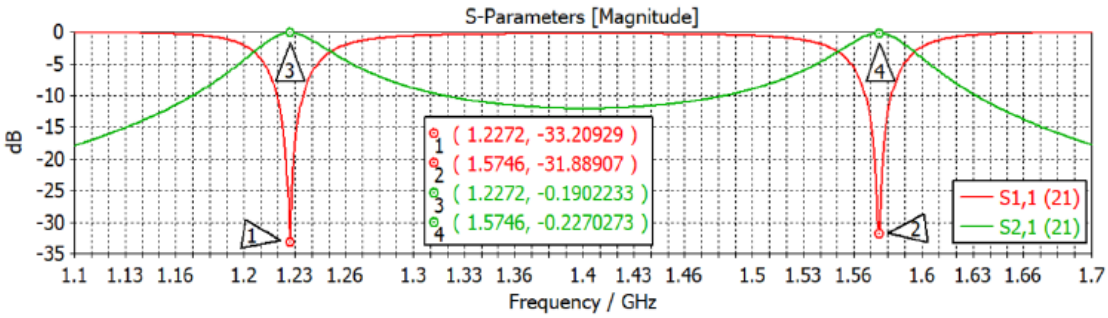

Figure 8. The simulated S_{11} and S_{21} of the dual 1-pole BPF with center frequencies of 1227 MHz and 1575 MHz.

2.3. Cascading Scheme

It should be noticed that, as shown in Figure 7, the dual 1-pole BPF should be an in-line structure. By simply cascading multiple of such structures to form a higher order DBPF, a long in-line structure is constructed. In order to reduce the length of the structure, it is recommended to 'bend' the structure using external coaxial cables. As shown in Figure 9, by carefully orientating the direction of the input

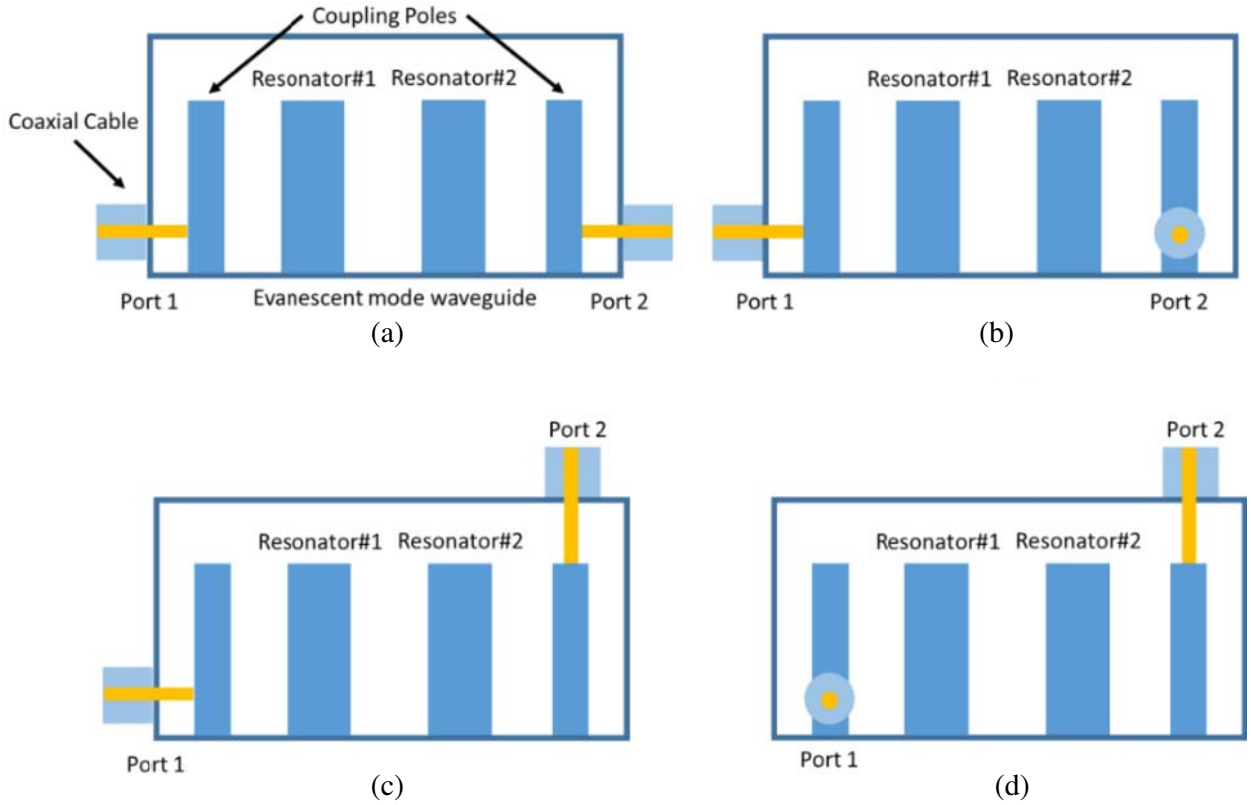

Figure 9. Four different orientations of input and output ports of the dual 1-pole BPF.

and output ports of the basic building block, the in-line structure can be folded vertically or horizontally without using any additional external coaxial cables. In other words, the final structure of the DBPF is constructed by stacking building blocks up or side by side. In this case, the length of the in-line structure can be reduced but at the expense of increasing height and width.

In addition to reducing the length of the structure, the proposed design technique can also help to reduce the total simulation time in the design phase by simultaneously designing and simulating multiple dual 1-pole BPF. In this case, the S-parameter of the complete filter can be obtained via CST 3D full wave EM/Circuit co-simulation, which can further reduce the simulation time. Furthermore, during the prototyping stage, all dual 1-pole BPF prototypes are allowed to be individually examined before cascading to form the final filter prototype. This can reduce the difficulties encountered in the post-tuning of high order filters. A dual 4-pole BPF is used to validate the proposed design concept.

2.4. Design Example: Dual 4-Pole BPF

In this example, a dual 4-pole BPF is designed based on the basic block as shown in Figure 7. The filter requirements for the dual 4-pole BPF are stated as follows.

Parameter	Specification
Number of Poles for each passband	4
Low passband frequency	1200 MHz to 1255 MHz
High passband frequency	1550 MHz to 1600 MHz
Reflection Coefficient	< -15 dB

The design procedure for the dual 4-pole BPF based on the proposed design technique is as follows.

i. Coupling Matrix: The coupling matrix of the dual 4-pole BPF is obtained using CST filter design as follows.

	S	1	2	3	4	5	6	7	8	L
S	0.000	0.574	0.000	0.000	0.000	0.000	0.000	0.000	0.000	0.000
1	0.574	0.000	1.013	0.000	0.000	0.000	0.000	0.000	0.000	0.000
2	0.000	1.013	0.000	0.278	0.000	0.000	0.000	0.000	0.000	0.000
3	0.000	0.000	0.278	0.000	0.977	0.000	0.000	0.000	0.000	0.000
4	0.000	0.000	0.000	0.977	0.000	0.227	0.000	0.000	0.000	0.000
5	0.000	0.000	0.000	0.000	0.227	0.000	0.977	0.000	0.000	0.000
6	0.000	0.000	0.000	0.000	0.000	0.977	0.000	0.278	0.000	0.000
7	0.000	0.000	0.000	0.000	0.000	0.000	0.278	0.000	1.013	0.000
8	0.000	0.000	0.000	0.000	0.000	0.000	0.000	1.013	0.000	0.574
L	0.000	0.000	0.000	0.000	0.000	0.000	0.000	0.000	0.574	0.000

ii. Evanescent mode waveguide selection: The dimension of the waveguide is 27 mm $\times$ 13 mm. It is chosen because the fundamental cutoff frequency is at 5.6 GHz, which is well above the highest frequency of the required DBPF.

iii. Capacitive structure design: A rectangular coaxial structure with embedded tuning screw (as shown in Figure 6) is used as the capacitive structure of the resonator.

iv. Stacking scheme and basic building block design: In this design, the Building Block #2 (BB#2) is designed to be stacked on top of Building Block #1 (BB#1) to form a dual 2-pole BPF. Then, the two dual 2-pole BPFs are connected side by side via a coaxial cable, as shown in Figure 10. With this arrangement, BB#1 and BB#2 are in the same form, as shown in Figure 9(d).

v. Basic building block design: The basic building block is a dual 1-pole BPF as shown in Figure 11. As per the coupling matrix suggested, two different building blocks are required, i.e., BB#1 and

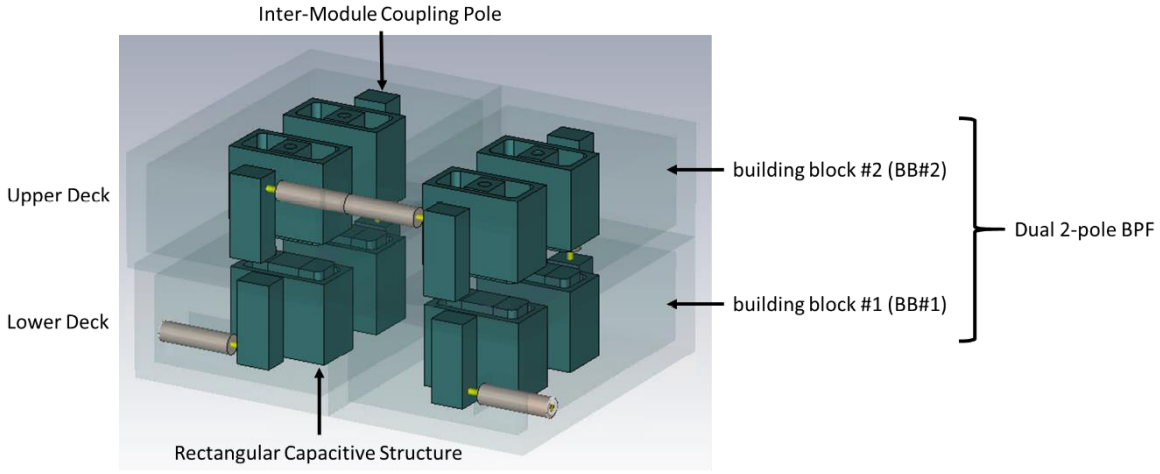

Figure 10. The stack scheme for the proposed dual 4-pole BPF.

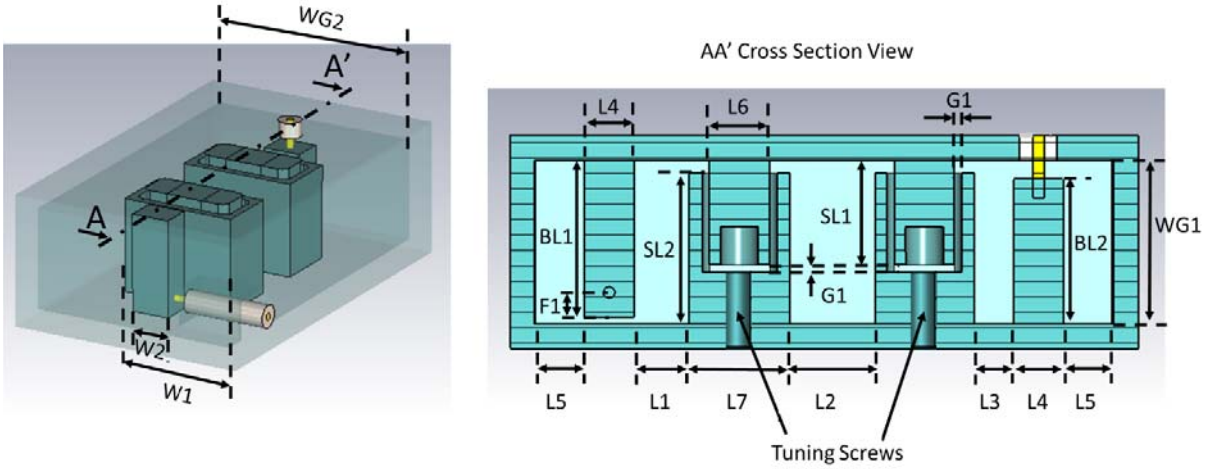

Figure 11. The building block (dual 1-pole BPF) for the proposed dual 4-pole BPF. Dimensions for BB#1(BB#2): $L1 = 2.7\,\text{mm}(4.4\,\text{mm})$, $L2 = 6.49\,\text{mm}(6.81\,\text{mm})$, $L3 = 3.1\,\text{mm}(3.1\,\text{mm})$, $L4 = L5 = 4\,\text{mm}(4\,\text{mm})$, $L6 = 4.8\,\text{mm}(4.8\,\text{mm})$, $L7 = 8\,\text{mm}(8\,\text{mm})$, $W1 = 15\,\text{mm}(15\,\text{mm})$, $W2 = 5\,\text{mm}(5\,\text{mm})$, $WG1 = 13\,\text{mm}(13\,\text{mm})$, $WG2 = 27\,\text{mm}(27\,\text{mm})$, $G1 = 0.6\,\text{mm}(0.6\,\text{mm})$, $BL1 = 12.5\,\text{mm}(12.5\,\text{mm})$, $BL2 = 11.5\,\text{mm}(11.5\,\text{mm})$, $SL1 = 8.3\,\text{mm}(8.3\,\text{mm})$, $SL2 = 12\,\text{mm}(12\,\text{mm})$ and $SL3 = 11.1\,\text{mm}(10.61\,\text{mm})$.

BB#2. BB#1 and BB#2 are in the same form, but the dimensions of their internal structures are slightly different, such as the distance between two resonators ($L2$), the distances between the coupling poles and resonators ($L1$ and $L3$), and the length of the fixed stub ($SL3$). The initial dimension of the BB#1 and BB#2 can be obtained based on the coupling matrix. The final dimensions for these two building blocks are shown in Figure 11.

vi. Simulation results: A total of two different basic building blocks (BB#1 and BB#2) are required, and they can be simulated simultaneously. In order to obtain the simulated S-parameter of the complete filter, the simulation results of BB#1 and BB#2 can be imported as 2-port network components and connected by wires in the circuit simulation (as shown in Figure 12). Using this co-simulation method, compared with 3D full wave simulation on the complete 3D filter model, the simulated S-parameter of the complete filter can be obtained much faster. In this example, it takes about 38 minutes to complete the 3D full-wave simulation of the dual 4-pole BPF (as shown in

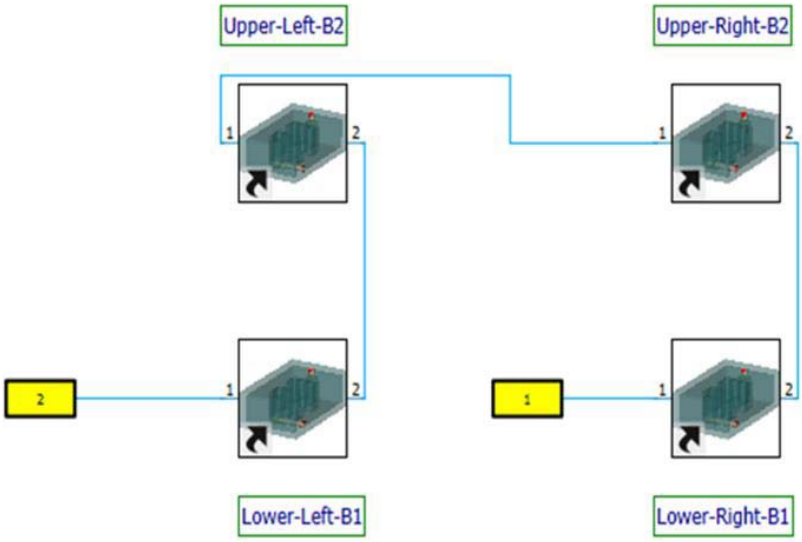

Figure 12. The circuit schematic of the dual 4-pole BPF using the S-parameter of the building blocks as a two port network.

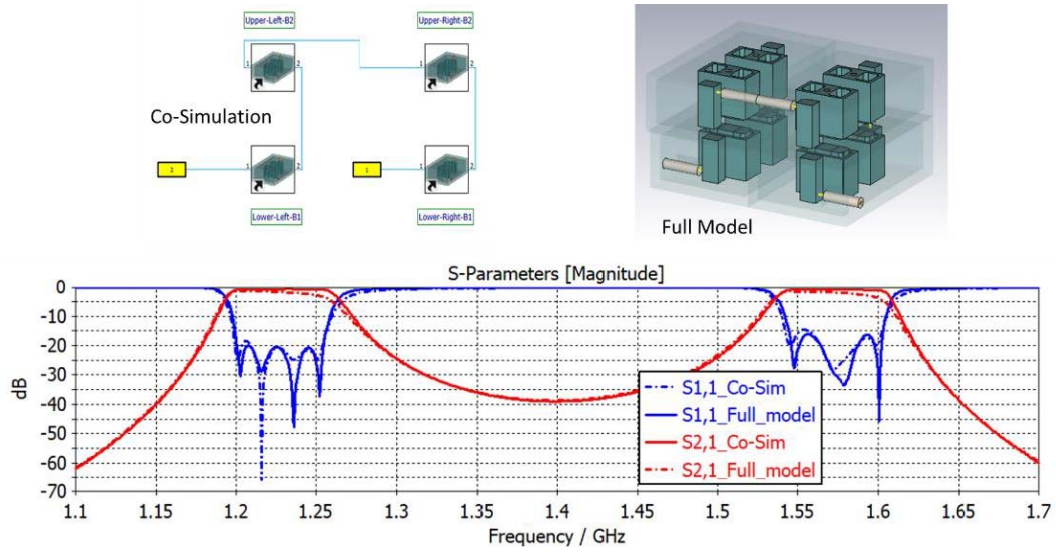

Figure 13. A comparison of the S-parameter simulation results of the proposed DBPF obtained via co-simulation and 3D full wave simulation.

Figure 13) in CST; it only takes 5 minutes to complete the 3D full wave simulation of the building blocks, while the circuit simulation only takes a few seconds. Therefore, the total simulation time is reduced by 6 times.

With several rounds of iterations, by using co-simulation method, the final simulated S-parameters of the proposed filter are obtained. All the critical dimensions for BB#1 and BB#2 are shown in Figure 9. For comparison, a complete filter model, as shown in Figure 13, is built and simulated. Figure 13 shows that these simulation results are in good agreement. As shown in Figure 14, the simulated stopband rejection level is better than 120 dB up to 5 GHz. The simulated S-parameters of BB#1 and BB#2 are shown in Figure 15. These simulated results are used as a reference during the prototype post tuning stage.

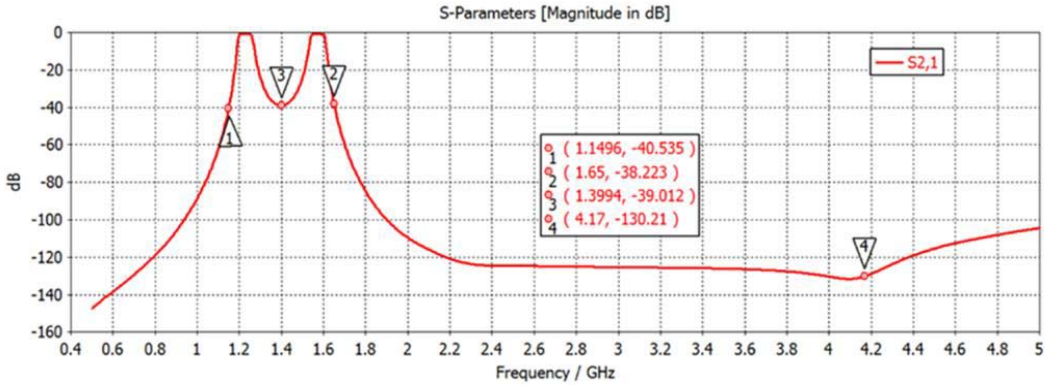

Figure 14. The S_{21} simulation result of the proposed DBPF.

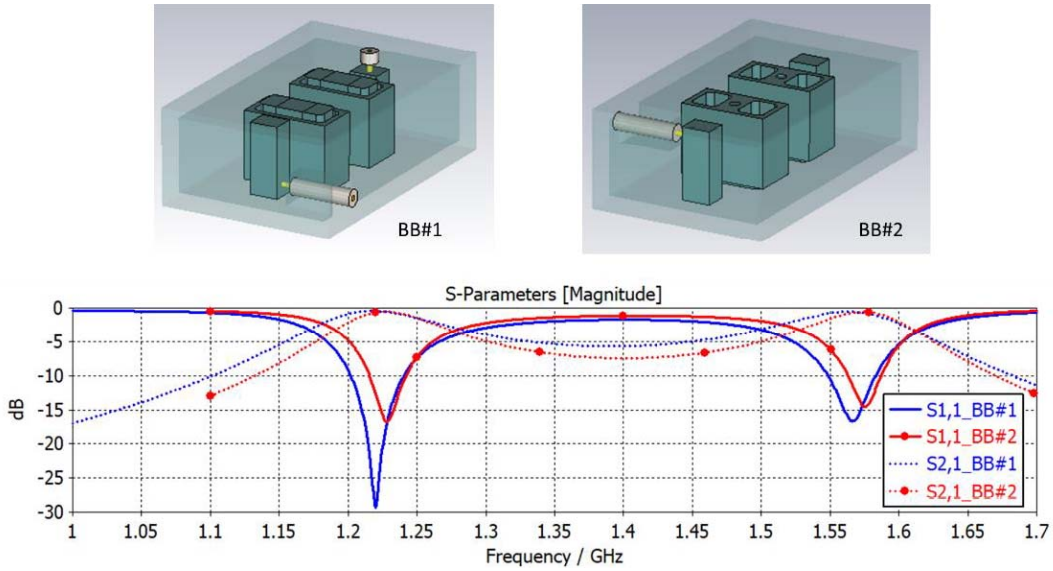

Figure 15. The simulated S-parameter plots for building block #1 (BB#1) and building block #2 (BB#2).

3. EXPERIMENTAL VERIFICATION

As shown in Figure 16, a prototype of a dual 4-pole BPF is fabricated and used for experimental verification of simulation results. The building block (dual 1-pole BPF) consists of two parts, the cover and the main body. It is made of aluminium material. The complete building block is shown in Figure 16(b). By installing field replaceable SMA connectors on those interconnect ports, all four building blocks are tuned and measured separately.

By comparing the measurement and simulation results of these building blocks, as shown in Figure 17, it is shown that all building blocks have been tuned correctly. Then, these blocks are connected together by replacing the SMA connectors with coaxial cables. By stacking all building blocks according to a predefined stacking scheme, a complete DBPF prototype is constructed. No further tunings on the prototype are required. The measured and simulated results of the DBPF are shown in Figure 18. The simulated and measured results agree well.

The measured reflection coefficients of both passbands are below -15 dB. The insert losses measured at the low passband and high passband are 1.03 dB $\sim$ 2.00 dB and 1.02 dB to 1.75 dB, respectively. In addition, the stopband rejection level measured at 5 GHz is better than 80 dB. The overall size of the

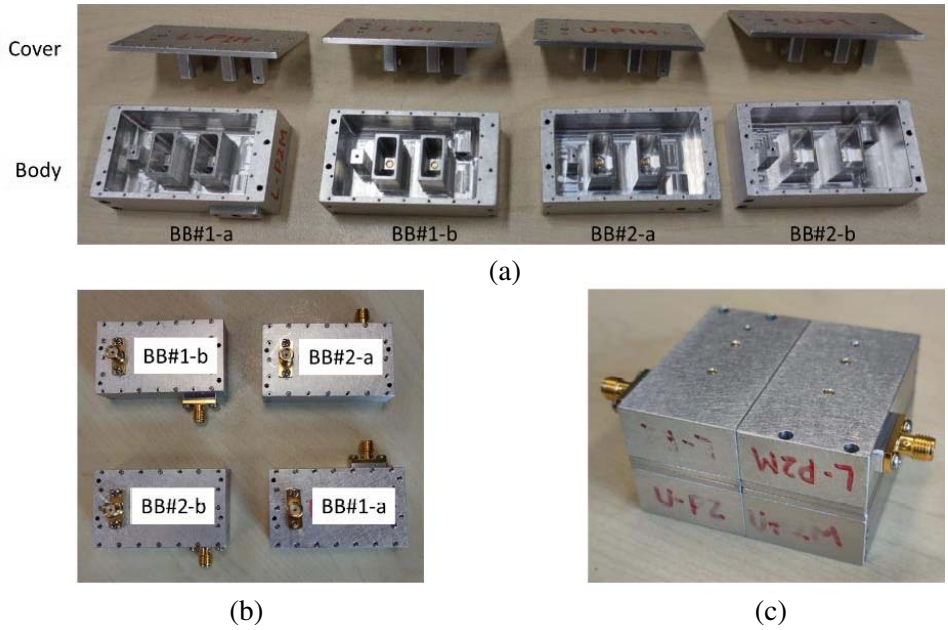

Figure 16. (a) Parts for the building blocks ($2\times$BB#1 and $2\times$BB#2), (b) BB#1 with SMA connector for individual S-parameter check, and (a) the fully assembled proposed dual 4-pole BPF prototype.

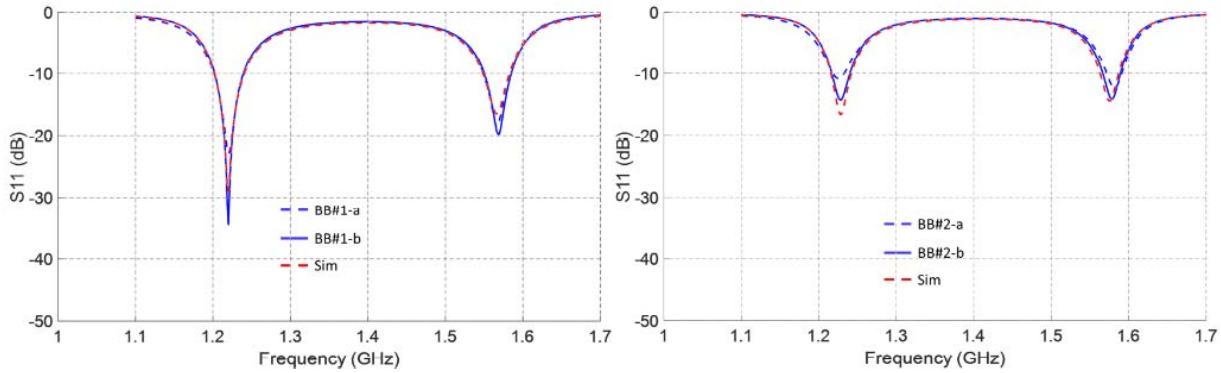

Figure 17. A comparison of simulated and measured S-parameter of the four dual 1-pole BPFs (BB#1-a, BB#1-b, BB#2-a and BB#2-b).

Table 1. The DBPF comparison table for some reference designs and the proposed 4-pole DBPF.

Design	Technique	Resonator Type	Order	Dimension (λ)			Volume	Centre Frequency (GHz)			Bandwidth(%)		Band Separation Ratio (BSR)
				Length	Width	Height	λ^3	Low Band (f_{c_LB})	High Band (f_{c_HB})	Between Two BPFs	Low Band	High Band	f_{c_HB}/f_{c_LB}
[9]	Dual-Resonance Structure	SIR	3	0.64	**0.21**	0.47	0.063	0.90	1.80	1.27	1.00	0.60	2.00
[11]	Transmission Zeros Insertion	Dual Mode Cylindrical Cavity	3	Not provided				20.95	21.06	21.00	0.10	0.10	1.01
[10]	Dual-Mode	Dual Mode Cylindrical Cavity	4	0.95	1.75	0.82	1.363	5.00	7.50	6.12	1.60	1.06	1.50
[7]	Frequency Transformation	Coaxial Resonator	4	0.68	0.34	0.25	0.057	2.51	2.56	2.53	0.80	0.78	1.02
Proposed	Strong Coupling	Evanescent mode cavity	4	**0.25**	0.29	**0.16**	**0.011**	1.23	1.58	1.39	3.60	4.20	1.28

DBPF prototype is 54.6 mm × 62 mm × 34 mm ($0.253\lambda \times 0.287\lambda \times 0.158\lambda$, where λ is the wavelength of the centre frequency between the two passbands, i.e., 1.39 GHz). For reference purpose, some reference designs [7, 9–11] are listed in Table 1 and compared with the proposed DBPF in terms of size and BSR.

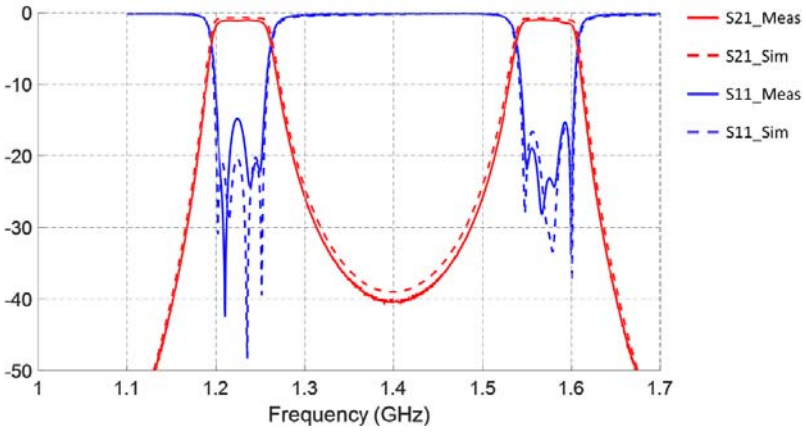

Figure 18. A comparison of simulated and measured S-parameter of the proposed DPBF.

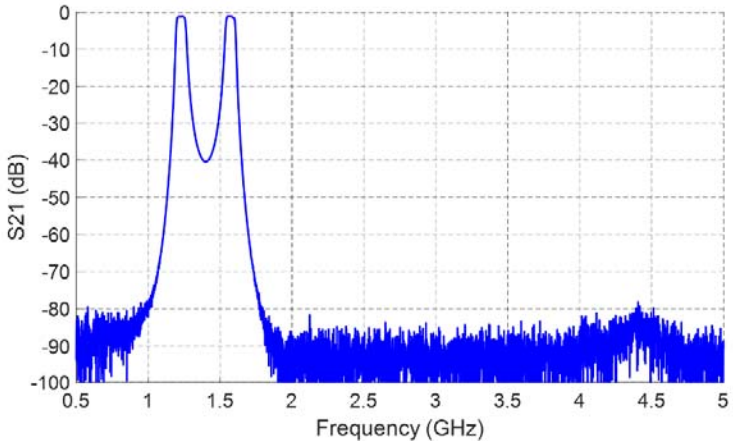

Figure 19. The measured S_{21} of the proposed DBPF from 0.5 GHz to 5 GHz.

4. CONCLUSIONS

In this paper, a new dual bandpass filter design is presented, where the dual resonance structure (or dual 1-pole BPF) or the building block is designed using the concept of strong coupling, and the high order DBPF is constructed by cascading these building blocks with appropriated couplings. In addition, it is recommended to stack these building blocks vertically and/or horizontally to obtain a compact form factor. By using this design concept, the simulation time in the design phase can be reduced significantly through the co-simulation method. Furthermore, each building block can also be examined individually prior to assembling them to form the high order DBPF. Therefore, it helps to simplify the post tuning process. However, by using strong coupling, Band Separation Ratio (BSR) is limited by the physically achievable coupling between the two resonators in the building block. A dual 4-pole BPF (1200 MHz to 1255 MHz and 1550 MHz to 1600 MHz) is designed based on the proposed method using evanescent mode waveguide with the dimension of 27 mm × 13 mm. A prototype of the designed filter is fabricated, and the measurement results are in good agreement with the simulated ones. In terms of insertion loss (1.03 dB $\sim$ 2.00 dB for low passband and 1.02 dB$\sim$1.75 dB for high passband), reflection coefficient (< -15 dB), and stopband rejection (> 80 dB up to 5 GHz), the overall performance of the prototype is considered satisfactory.

REFERENCES

1. Pozar, D. M., *Microwave Engineering*, John Wiley & Sons, 2009.
2. Cameron, R. J., C. M. Kudsia, and R. R. Mansour, *Microwave Filters for Communication Systems: Fundamentals, Design and Applications*, 2nd Edition, Wiley, Hoboken, NJ, USA, 2018.
3. Tsai, L.-C. and C.-W. Hsue, "Dual-band bandpass filters using equal-length coupled-serial-shunted lines and Z-transform technique," *IEEE Transactions on Microwave Theory and Techniques*, Vol. 52, No. 4, 1111–1117, 2004.
4. Sekar, V. and K. Entesari, "A novel compact dual-band half-mode substrate integrated waveguide bandpass filter," *IEEE MTT-S International Microwave Symposium Digest. IEEE MTT-S International Microwave Symposium*, 1–4, 2011.
5. Wu, Y., "Compact microwave dual-band bandpass filter design," University of York, 2017.
6. Chen, J. and X. Liu, "Design of an evanescent-mode tunable dual-band filter," *2016 IEEE/MTT-S International Microwave Symposium — MTT*, 2016.
7. Kou, X., Z.-Y. Xiao, C.-Y. Huang, H. Li, and J.-J. Chu, "Design of dual-band cavity filter using frequency transformation method," *Journal of Electronics & Information Technology*, Vol. 34, 1489–1493, 2012.
8. Chomtong, P. and P. Akkaraekthalin, "A dual-band cavity bandpass filter using interdigital technique," *ECTI 2015*, 261–264, 2015.
9. Chen, F.-C., J.-M. Qiu, S.-W. Wong, and Q.-X. Chu, "Dual-band coaxial cavity bandpass filter with helical feeding structure and mixed coupling," *IEEE Microwave and Wireless Components Letters*, Vol. 25, No. 1, 31–33, 2014.
10. Naeem, U., A. Perigaud, and S. Bila, "Dual-mode dual-band bandpass cavity filters with widely separated passbands," *IEEE Transactions on Microwave Theory and Techniques*, Vol. 65, No. 8, 2681–2686, 2017.
11. Lee, J., M. S. Uhm, and I.-B. Yom, "A dual-passband filter of canonical structure for satellite applications," *IEEE Microwave and Wireless Components Letters*, Vol. 14, No. 6, 271–273, 2004.
12. Stefanovski, S., M. Potrebic, D. Toic, and Z. Stamenkovic, "A novel compact dual-band bandpass waveguide filter," *2015 IEEE 18th International Symposium on Design and Diagnostics of Electronic Circuits & Systems*, 51–56, 2015.
13. Stefanovski, S., M. Potrebić, D. Tošić, and Z. Stamenković, "Compact dual-band bandpass waveguide filter with H-plane inserts," *Journal of Circuits, Systems and Computers*, Vol. 25, No. 3, 1640015, 2016.
14. Macchiarella, G. and S. Tamiazzo, "Design techniques for dual-passband filters," *IEEE Transactions on Microwave Theory and Techniques*, Vol. 53, No. 11, 3265–3271, 2005.
15. Almorqi, S., H. Shaman, J. S. Hong, and O. M. Haraz, "Design of a compact dual-band folded-waveguide bandpass filter using multilayer waveguide resonators," *International Journal of RF and Microwave Computer-Aided Engineering*, Vol. 25, No. 9, 780–788, 2015.
16. "CST Computer Simulation Technology AG," https://www.cst.com/.
17. Jarry, P. and J. Beneat, *Advanced Design Techniques and Realizations of Microwave and RF Filters*, Wiley Online Library, 2008.
18. Craven, G. F. and C. Mok, "The design of evanescent mode waveguide bandpass filters for a prescribed insertion loss characteristic," *IEEE Transactions on Microwave Theory and Techniques*, Vol. 19, No. 3, 295–308, 1971.